



Deep Brain Stimulation Modulates Multiple Abnormal Resting-State Network Connectivity in Patients With Parkinson's Disease

Yutong Bai¹, Yu Diao¹, Lu Gan², Zhizheng Zhuo², Zixiao Yin¹, Tianqi Hu¹, Dan Cheng², Hutaio Xie¹, Delong Wu¹, Houyou Fan¹, Quan Zhang¹, Yunyun Duan², Fangang Meng¹, Yaou Liu^{2*}, Yin Jiang^{3*} and Jianguo Zhang^{1,3,4*}

OPEN ACCESS

Edited by:

Ignacio Torres-Aleman,
Achucarro Basque Center
for Neuroscience, Spain

Reviewed by:

Radhika Madhavan,
GE Global Research, United States
Paola Valsasina,
San Raffaele Scientific Institute,
Scientific Institute for Research,
Hospitalization and Healthcare
(IRCCS), Italy

*Correspondence:

Yaou Liu
yaouliu80@163.com
Yin Jiang
jiangyin0802@foxmail.com
Jianguo Zhang
ziguoz73@126.com

Specialty section:

This article was submitted to
Parkinson's Disease
and Aging-related Movement
Disorders,
a section of the journal
Frontiers in Aging Neuroscience

Received: 14 October 2021

Accepted: 08 February 2022

Published: 21 March 2022

Citation:

Bai Y, Diao Y, Gan L, Zhuo Z,
Yin Z, Hu T, Cheng D, Xie H, Wu D,
Fan H, Zhang Q, Duan Y, Meng F,
Liu Y, Jiang Y and Zhang J (2022)
Deep Brain Stimulation Modulates
Multiple Abnormal Resting-State
Network Connectivity in Patients With
Parkinson's Disease.
Front. Aging Neurosci. 14:794987.
doi: 10.3389/fnagi.2022.794987

¹ Department of Neurosurgery, Beijing Tiantan Hospital, Capital Medical University, Beijing, China, ² Department of Radiology, Beijing Tiantan Hospital, Capital Medical University, Beijing, China, ³ Department of Neurosurgery, Beijing Neurosurgical Institute, Beijing, China, ⁴ Beijing Key Laboratory of Neurostimulation, Beijing, China

Background: Deep brain stimulation (DBS) improves motor and non-motor symptoms in patients with Parkinson's disease (PD). Researchers mainly investigated the motor networks to reveal DBS mechanisms, with few studies extending to other networks. This study aimed to investigate multi-network modulation patterns using DBS in patients with PD.

Methods: Twenty-four patients with PD underwent 1.5 T functional MRI (fMRI) scans in both DBS-on and DBS-off states, with twenty-seven age-matched healthy controls (HCs). Default mode, sensorimotor, salience, and left and right frontoparietal networks were identified by using the independent component analysis. Power spectra and functional connectivity of these networks were calculated. In addition, multiregional connectivity was established from 15 selected regions extracted from the abovementioned networks. Comparisons were made among groups. Finally, correlation analyses were performed between the connectivity changes and symptom improvements.

Results: Compared with HCs, PD-off showed abnormal power spectra and functional connectivity both within and among these networks. Some of the abovementioned abnormalities could be corrected by DBS, including increasing the power spectra in the sensorimotor network and modulating the parts of the ipsilateral functional connectivity in different regions centered in the frontoparietal network. Moreover, the DBS-induced functional connectivity changes were correlated with motor and depression improvements in patients with PD.

Conclusion: DBS modulated the abnormalities in multi-networks. The functional connectivity alterations were associated with motor and psychiatric improvements in PD. This study lays the foundation for large-scale brain network research on multi-network DBS modulation.

Keywords: Parkinson's disease, deep brain stimulation, resting-state network, functional connectivity, power spectra, frontoparietal network

INTRODUCTION

Deep brain stimulation (DBS) is a promising treatment in patients with moderate-to-advanced Parkinson's disease (PD) (Krauss et al., 2021; Yin et al., 2021b). DBS can significantly improve motor and non-motor symptoms (Mansouri et al., 2018; Cartmill et al., 2021; Diao et al., 2021; Yin et al., 2021a), although the neuromodulation mechanism of DBS is still unclear.

Studies of DBS-modulated abnormal neurocircuits have mainly focused on the motor network. In neuroimaging studies, it is generally believed that functional connectivity declines within sensorimotor networks (SMNs) in patients with PD, when compared with healthy controls (HCs) (Suo et al., 2017; Ji et al., 2018). Functional connectivity changes in the SMN and basal ganglia network correlate with motor severity (Manza et al., 2016). DBS increased the effective connectivity in the direct pathways, which led to decoupling of the functional connectivity in the subthalamic nucleus (STN) (Kahan et al., 2019). In electrophysiological studies, similar results have also been reported, namely, DBS excited local neuron activity, which inhibited synchronization between basal ganglia and the primary motor cortex (M1) (Wichmann and DeLong, 2016). All these studies showed that DBS improved the efficiency of information transmission in the thalamus (Molnar et al., 2005). This phenomenon increases the excitability of the primary motor cortex (M1), to improve motor symptoms (Johnson et al., 2020).

Still, studies of modulating abnormal neurocircuits in multi-networks by DBS are limited. It has been reported that patients with PD had multi-network impairments when compared with controls (Mohan et al., 2016). The non-motor symptoms in PD are closely related to functional connectivity changes in multi-networks (Tinaz, 2021). Clinical studies showed that DBS significantly improved PD non-motor symptoms (Petry-Schmelzer et al., 2019; Diao et al., 2021; Yin et al., 2021a). However, the modulation patterns of DBS in multi-networks remain unclear. The responses between dopaminergic drugs and DBS in symptom improvements are comparable (Mueller et al., 2018). Previous studies showed that dopaminergic drugs (medication on) partially normalized PD-related functional connectivity patterns in multi-networks when compared with nondrug states (medication off) (Tinaz, 2021). Accordingly, we hypothesized that DBS may also modulate functional connectivity in a multi-network manner.

In this study, we aimed to characterize the multiple resting-state network (RSN) alteration patterns using DBS modulation. We obtained resting-state functional MRI (rs-fMRI) data from patients with PD after stable DBS, by comparing differences within and between networks among different groups.

MATERIALS AND METHODS

Participants

A total of 40 patients from the Department of Neurosurgery, Beijing Tiantan Hospital, were enrolled in this study. The inclusion criteria were as follows: (1) diagnosed with idiopathic PD according to the UK Brain Bank Clinical Criteria, (2)

implanted with bilateral STN-DBS (Medtronic 3389; Medtronic, Dublin, Ireland) for at least 3 months, (3) Hoehn-Yahr (H&Y) stage 2.5–4.0 in medication-off, and (4) preoperative medication improvement rate higher than 30%. The exclusion criteria were as follows: (1) severe head tremors, (2) combining with other neurological diseases, (3) unilateral lead implantation, and (4) implantation of an internal pulse generator (IPG) in the right chest. We also enrolled 28 age-matched HCs. This study was approved by the Institutional Review Board of Beijing Tiantan Hospital of Capital Medical University (Approval Number: KY 2018-008-01). All participants provided written informed consent. More than 20 subjects for PD and HC were enrolled because a sample size ≥ 20 was recommended for sufficient reliability in fMRI studies (Thirion et al., 2007). The experimental protocol adhered to the tenets of the Declaration of Helsinki.

Clinical Evaluation

The flowchart of this study is illustrated in **Supplementary Figure 1**. The optimal parameters were programmed by experienced clinicians within 1 week of scans. Patients were required to withdraw their medications overnight on the day before scanning. On the day of scanning, patients were assigned by using a pseudorandom method into two balanced scanning pathways. In one pathway, patients first received scanning in the DBS-on state, while the motor functions were evaluated immediately after scanning (stim-on/med-off). Then, the DBS was switched off, and the patients waited for 2 h or until the motor symptoms reappeared. Patients received scans for the second time in the DBS-off state, while the motor functions were evaluated immediately after scanning (stim-off/med-off). In the other pathway, the order of scanning was swapped, to minimize bias from poststimulus effects (Zhang et al., 2021).

Motor functions were evaluated using the Movement Disorder Society Unified Parkinson's Disease Rating Scale part III (MDS-UPDRS-III). MDS-UPDRS-III contained four domains (Stenmark Persson et al., 2021), namely, tremor (items 15–18), rigidity (item 3), bradykinesia (items 2, 4–8, and 14), and axial (items 1 and 9–13). The Hamilton Depression Scale (HAM-D) and the Hamilton Anxiety Scale (HAM-A) were used to assess the severity of both preoperative and postoperative mood disorders.

MRI Acquisition

Participants were scanned using a 1.5-T GE SIGNA Explorer MRI scanner (General Electric, San Ramon, CA, United States). We acquired the rs-fMRI data in two states as described above. Structural images were conducted by using the magnetization-prepared rapid acquisition gradient echo sequence: repetition time (TR) = 1,146 ms, echo time (TE) = 4.97 ms, flip angle (FA) = 12°, voxel size = 1 mm \times 1 mm \times 0.7 mm, slices = 286, field of view (FOV) = 240 mm \times 240 mm, and matrix size = 256 mm \times 256 mm. The blood-oxygen-level-dependent (BOLD) image was obtained using the following echo-planar imaging sequence: TR = 3,000 ms, TE = 40 ms, FA = 90°, acquisition matrix = 64 \times 64, number of slices = 36, voxel size = 3.75 mm \times 3.75 mm \times 4 mm, slice gap = 1 mm, FOV = 240 mm \times 240 mm, and scanning time \approx 7 min.

Artifact Filling and Preprocessing of fMRI Data

The MRI scans after DBS suffered from magnetic susceptibility artifacts caused by the DBS apparatus, which reduced the accuracy of normalization (Holiga et al., 2015). All patients' IPG were in the left chest, so all artifacts were in the left brain. The artifact areas included the partial left inferior parietal lobe, left temporal lobe, left occipital lobe, and left cerebellum. We used enantiomorphic normalization methods (mirror image normalization) to fill the artifact. The signal from the contralateral region (symmetry around the midline), specifically, is filled to the artifact region (Nachev et al., 2008; Yourganov et al., 2016; Keller et al., 2017). Thus, the artifact-filled images were better normalized to the Montreal Neurological Institute (MNI) space (Figure 1). The filled signals in these artifact regions were excluded for further analysis.

The artifact-filled images were preprocessed using SPM12¹. Functional images were preprocessed according to a standard pipeline: (a) the first five time points (15 s) were removed; (b) scans were slice-time-corrected to the median (35th) slice in each TR; and (c) scans were then realigned to create a mean realigned image. Participants with head motions exceeding 3 mm or 3° of rotation in any direction were excluded. (d) Two-step normalization: T1 structural images were co-registered to rs-fMRI images using a nonlinear image registration approach and to automatically segment the brain into different ingredients. (e) Scans were spatially smoothed using 6 mm × 6 mm × 6 mm full width at half maximum (FWHM).

Independent Component Analysis

Single-subject and group-level independent component analysis (ICA) was conducted using the Infomax algorithm using Group ICA of the fMRI Toolbox (GIFT V4.0)². The number of independent components (ICs) were estimated using the minimum description length (MDL) criteria, and 20 ICs were extracted for each subject (Calhoun et al., 2001). Stability was assessed using ICASSO with 20 repetitions (Himberg et al., 2004). After back reconstruction, the spatial components were converted to *z*-scores in each single subject (*z*-maps). The components were identified by spatially sorting all components with the healthy volunteer anatomy masks of RSNs (Smith et al., 2009). Default mode network (DMN), SMN, right frontoparietal networks (r-FPN), salience network (SN), and left frontoparietal network (l-FPN) were extracted for further analyses (Supplementary Figure 2). The *z*-maps of selected components were submitted to a group-specific one-sample *t*-test, with cluster-wise false discovery rate (FDR) correction for multiple comparison, to describe each selected RSNs. For each network, the utility of spectral group comparison in the GIFT was used to compare the difference of power spectra of 0.01–0.08 Hz between groups. The functional connectivity among networks was also compared by using the MANCOVAN toolbox in Group ICA.

¹<https://www.fil.ion.ucl.ac.uk/spm>

²<http://icatb.sourceforge.net/>

Region of Interest Identification and Analysis of Functional Connectivity Among Resting-State Networks

To further observe the region-to-region connectivity, region of interest (ROI)-based connectivity analyses were performed. After temporally detrend, band-pass filter (0.01–0.08 Hz) and regress out covariates (white matter, cerebrospinal fluid (CSF) signal, and head motion), fifteen ROIs in the five abovementioned networks were selected (Yeo et al., 2014), including the medial prefrontal cortex (mPFC), posterior cingulate cortex (PCC), right inferior parietal lobule (r-IPL) in DMN, supplementary motor area (SMA), left primary motor cortex (l-M1), and right primary motor cortex (r-M1) in the SMN; anterior cingulate cortex (ACC), left insula (l-INS), and right insula (r-INS) in the SN; left premotor area (l-PMA), left dorsolateral prefrontal cortex (l-dlPFC), and left posterior parietal cortex (l-PPC) in the l-FPN; right premotor area (r-PMA), right dorsolateral prefrontal cortex (r-dlPFC), and right posterior parietal cortex (r-PPC) in the r-FPN.

For each ROI, BOLD signal time courses in each scan were extracted within a 6-mm sphere with the center localized at the peak voxel (the highest *t*-value after one-sample *t*-test for its component) (Supplementary Figure 3). Correlations among ROIs were calculated using Pearson's correlation. For each subject in each scan, there was a matrix containing all the correlation coefficients (*r*-values) among the ROIs. The *r*-value matrices among HC, PD-off, and PD-on were compared, with age and sex regressed as covariates.

Resting-State Network Behavioral Correlation

The correlation between functional connectivity changes and the clinical scores' change rate (MDS-UPDRS-III total score; tremor, rigidity, bradykinesia, and axial subscores; HAM-A and HAM-D scores) was assessed using Pearson's correlation. A univariable linear regression model was used to draw the best-fit line with the threshold of *P* < 0.05.

The motor change rate was calculated as follows:

$$\frac{(\text{PD-off scores}) - (\text{PD-on scores})}{(\text{PD-off scores})} \times 100\%$$

The mood change rate was calculated as follows:

$$\frac{(\text{preoperative scores}) - (\text{postoperative scores})}{(\text{preoperative scores})} \times 100\%$$

Statistical Analysis

Data were presented as mean ± SD or median (Q1, Q3) for continuous variables and percentage for binary variables. All variables were tested for normality by using the Anderson-Darling normality test. Comparisons between groups (HC vs. PD-off and HC vs. PD-on) were performed by the independent *t*-tests for continuous variables with the normal distribution and by the Mann-Whitney *U* test for continuous variables with the skew distribution. Comparisons of repeated measurements (PD-off vs. PD-on) were performed by the paired *t*-tests for

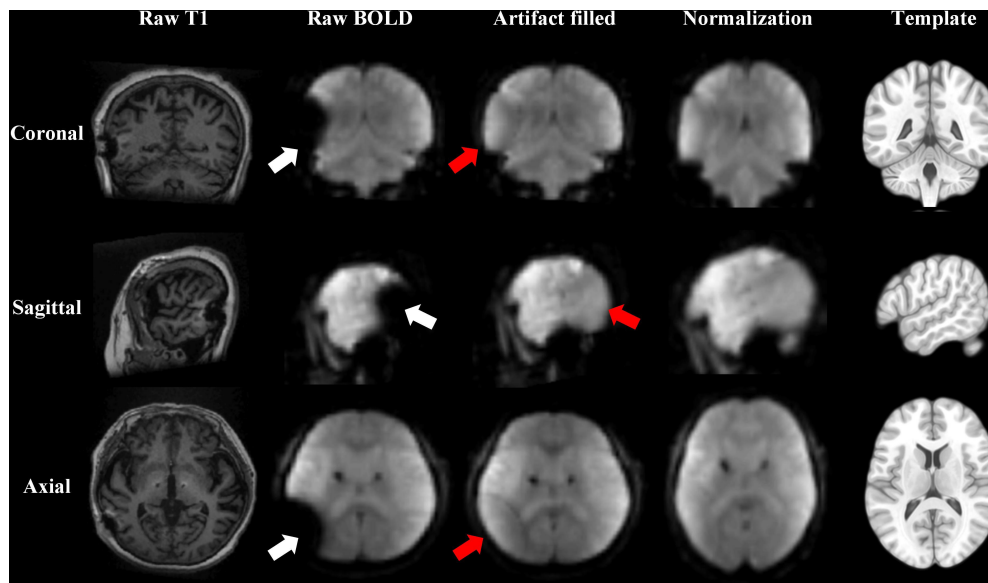


FIGURE 1 | Resting-state fMRI data preprocessed after the deep brain stimulation (DBS) artifact was filled. An enantiomorphic normalization method was used to fill the artifacts of the raw blood-oxygen-level-dependent (BOLD) data, to improve the accuracy of normalization to the Montreal Neurological Institute (MNI) space. The white arrow shows the artifact lesion. The red arrow shows the filled lesion. The results are displayed from coronal, sagittal, and axial views in three rows. The columns show the raw T1 image, raw BOLD image, and BOLD image after the artifacts were filled; the BOLD image after normalization; and the MNI template from left to right.

continuous variables with the normal distribution and by the Wilcoxon matched-pairs signed-rank test for continuous variables with the skew distribution. The chi-square test was used for binary variables, and Pearson's correlation was used for correlation analysis. The multiple comparison test was performed by FDR, and the corrected $P < 0.05$ was considered significant. All statistical analysis was conducted using SPSS 24 (IBM, Chicago, IL, United States) and Python 3. Images were drawn using GraphPad Prism 9.0 (GraphPad Software, San Diego, CA, United States).

RESULTS

Clinical Motor and Psychology Findings

All participants were right-handed, without resting head tremors. A total of 17 patients were excluded, including 13 with excessive head movements (one in the HC group), and 4 intolerant to scanning. The remaining 24 patients with PD (62.5 ± 7.9 years, 15 men) and 27 HCs (61.6 ± 4.6 years, 14 men) were included for further analyses. Individual data for all patients with PD are listed in **Supplementary Table 1**. There was no significant difference in age and sex between the HCs and patients with PD. In patients with PD, the disease duration was 10.9 ± 3.2 years, the H&Y stage was 2.9 ± 0.2 at med-off preoperatively, and the levodopa equivalent doses were 661.6 ± 258.7 mg. The mean follow-up was 18.0 ± 17.6 months after DBS surgery. The comparison between baseline characteristics is shown in **Table 1**. DBS significantly improved not only overall motor performance and all motor subscores but also depression and anxiety.

Identification and Power Spectra Changes Among Resting-State Networks

Five components were identified as RSNs of interest. These RSNs were DMN, l-FPN, r-FPN, SMN, and SN (**Figure 2A**, $P < 0.05$, FDR-corrected). The composition and location of each RSN were similar to the templates. The components in each group are

TABLE 1 | Baseline characteristics of the enrolled sample.

	Patients (n = 24)	Controls (n = 27)	P-value
Age	62.5 ± 7.9	61.6 ± 4.6	0.617
Gender / Man	62.5%	51.9%	0.443
Disease Duration	10.9 ± 3.2	-	
	PD-off ^a	PD-on ^a	
MDS-UPDRS-III	44.7 ± 16.3	22.3 ± 9.9	$< 0.001^*$
Tremor	8.4 ± 5.8	3.5 ± 3.0	$< 0.001^*$
Rigidity	7.5 ± 2.7	3.4 ± 2.0	$< 0.001^*$
Bradykinesia	20.5 ± 8.9	10.4 ± 5.7	$< 0.001^*$
Axial	9.3 ± 4.8	5.4 ± 3.4	$< 0.001^*$
HAM-D ^b	16.9 ± 9.4^c	12.8 ± 7.9^d	$< 0.001^*$
HAM-A ^b	16.9 ± 10.1^c	11.8 ± 6.4^d	$< 0.001^*$

Data were presented as the mean \pm SD. PD-on and PD-off indicate the DBS status.

*Statistics significant difference.

^aAll data were collected during medication withdrawn for at least 12 h.

^bHAM-D and HAM-A were collected in 20 patients.

^cPreoperative scores.

^dLast follow-up scores.

shown in **Supplementary Figure 2**. The power spectra in SMN significantly decreased in PD-off compared with HC, while PD-on was significantly increased (HC vs. PD-off: -0.22 , $P < 0.001$; PD-on vs. PD-off: -0.12 , $P = 0.030$). The power spectra in SN significantly increased in PD-off compared with HC, with a decreasing trend seen in the PD-on (HC vs. PD-off: 0.21 , $P = 0.009$; PD-on vs. PD-off: -0.09 , $P = 0.339$). No significant difference was found in other networks (**Figure 2D**).

Functional Network Connectivity Changes Among Resting-State Networks

In network analysis, compared with HC, PD-off showed decreased connectivity in DMN/SMN ($t = 3.81$, $P < 0.001$), DMN/r-FPN ($t = -3.16$, $P = 0.003$), SN/r-FPN ($t = 4.03$, $P < 0.001$), and SN/l-FPN ($t = 3.68$, $P < 0.001$), while PD-on showed decreased connectivity in DMN/SMN ($t = 2.63$, $P = 0.011$), SN/r-FPN ($t = 3.20$, $P = 0.002$), and SN/l-FPN ($t = 3.56$, $P = 0.001$). No significant difference was found in network connectivity between PD-on and PD-off (**Figures 2B,C**).

Furthermore, in the ROI analysis, the mean functional connectivity matrix constructed by 15 ROIs for HC, PD-off, and PD-on was calculated by averaging the individual matrices and was shown in **Figure 3A**. A significantly changed functional connectivity between HC and PD-off is shown in **Figure 3B** (left, contralateral results; right, ipsilateral results). Most of the abnormal functional connectivities decreased in PD-off compared with HC, except the functional connectivity in r-PPC/r-IPL. The abnormal functional connectivity reversed by DBS is shown in **Figure 4**. All reversed functional connectivities were ipsilateral. The functional connectivity increased within SMN (SMA/l-M1 and SMA/r-M1), between FPN and SMN (l-PMA/l-M1 and r-PMA/r-M1), SN (l-PPC/ACC and r-PPC/ACC), and DMN (l-dIPFC/mPFC). The functional connectivity decreased between r-IPL/r-PPC. The statistical measures of the abovementioned functional connectivity are shown in **Supplementary Table 2**. **Supplementary Figure 4** shows the abnormal functional connectivity, which could not be reversed by DBS. All results were FDR-corrected.

Behavioral Correlations of Resting-State Networks

The functional connectivity changes between ROIs were correlated with the change rate of MDS-UPDRS-III total scores, subscores in each domain (tremor, rigidity, bradykinesia, and axial), and HAM-D and HAM-A scores (**Figure 5**).

Specifically, a positive correlation with the change rate of MDS-UPDRS-III total score was found in the functional connectivity changed in SMA/l-M1, SMA/r-M1, l-PMA/l-M1, and r-PMA/r-M1. Positive correlations with the change rate of tremor subscores were observed in the functional connectivity changes in r-PMA/r-M1, l-PMA/l-M1, and SMA/l-M1.

We also observed some tendency results, with uncorrected $P < 0.05$, but not survived after FDR correction, including (1) the change rate of rigidity subscore was a positive correlation with the functional connectivity changes in l-PMA/l-M1; (2) the change rate of axial subscore was a positive correlation with the

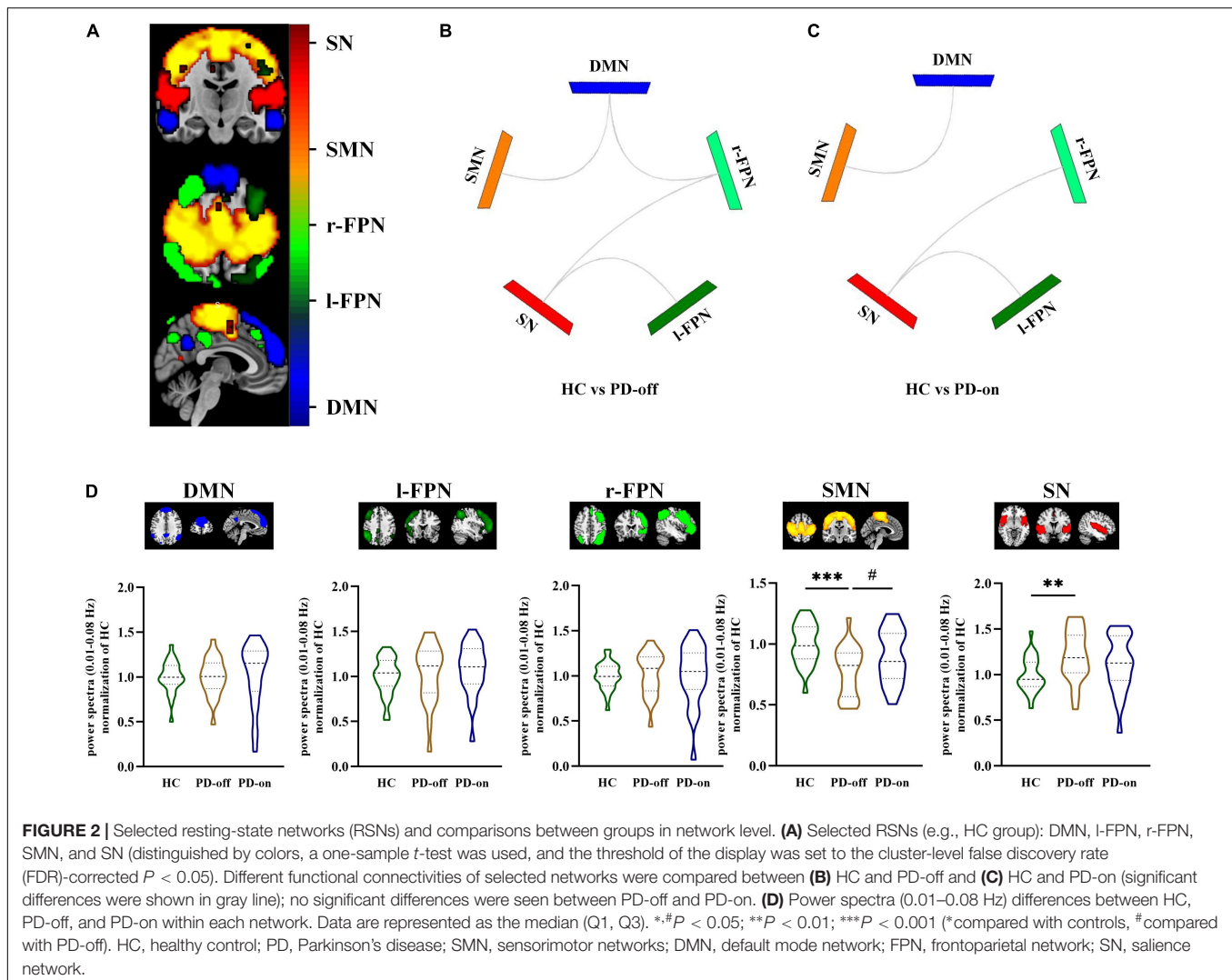
functional connectivity changes in SMA/r-M1; and (3) the change rate of HAM-D was a positive correlation with l-PPC/ACC and r-PPC/ACC.

DISCUSSION

The first finding of this study was that SMN was a key network in DBS modulation, which involved modulation patterns within this network. Specifically, DBS reversed power spectra declines in SMN and increased abnormal functional connectivity within SMN. Power spectra describe the brain activity at 0.01–0.08 Hz in special brain networks, acting as an important biomarker reflecting intra-network intensities. These findings were consistent with previous studies. Horn et al. reported that DBS increased functional connectivity in the cerebello-thalamo-cortical network (Horn et al., 2019). Kahan et al. (2014) further clarified the DBS modulation effect on information flow within motor networks. STN-DBS inhibited the indirect pathway and excited the direct pathway, resulting in enhanced thalamic excitability, which increased primary motor cortex activity and accelerated the information flow in motor networks (Kahan et al., 2014, 2019).

For the inter-network differences, an interesting finding was that DBS was not effective to modulate the functional connectivity between different networks, but it was effective to modulate the functional connectivity between representative brain regions in each network. This suggested that DBS did not reverse the decoupling among networks in patients with PD but partially improved the inter-network connections by modulating the core brain regions within each network. This indicated the limitations of DBS for network modulation. Wu et al. noted that STN-DBS did not improve global network measures but was negatively associated with network assortativity (Wu et al., 2021), which consisted with our findings.

Another finding of the study was that the FPN also played an important role in DBS modulation. The functional connectivity between regions in FPN with other networks was modulated by DBS. The FPN is a top-down network, which allows the modulation of information processing from top to bottom in other brain regions to facilitate executive control and adaptive behavior (Dixon et al., 2018; Chen et al., 2021). In PD, the abnormal functional connectivity associated with FPN is usually inter-network (Tinaz, 2021). Similarly, we found that the abnormal functional connectivity in PMA/M1, r-IPL/r-PPC, l-dIPFC/mPFC, and PPC/ACC could be modulated by DBS. (1) DBS modulated the functional connectivity in PMA/M1, which reflected motor performance (Lam et al., 2018). Vervoort et al. reported that functional connectivity decreased between SMN and FPN in patients with PD when compared with controls (Vervoort et al., 2016). A dynamic functional network study also reported that the fractional window in FPN/SMN was reduced in patients with PD when compared with HCs, suggesting a reduced cross-talk between the two networks (Chen et al., 2021). This was closely associated with motor deficits in PD. Our results showed that DBS increased functional connectivity between the PMA and M1. This may increase the information transmission



between networks, further improving motor symptoms. (2) DBS modulated the functional connectivity in the PPC/ACC, which reflected mood fluctuations (Lou et al., 2015). Hu et al. reported decreased functional connectivity between frontal-limbic regions in patients with PD with depression when compared with those without depression (Hu et al., 2015). Our results showed that DBS increased functional connectivity between PPC and ACC, which reversed the abnormal functional connectivity in patients with PD. (3) DBS modulated the functional connectivity in the regions of FPN/DMN, which was related to multiple neural events. Mohan et al. (2016) reported that abnormal changes between FPN and DMN were considered as disease-related network disruptions. Alterations in functional connectivity between FPN and DMN are associated with several non-motor symptoms in patients with PD, such as cognitive impairment (Lang et al., 2019), hallucination (Bejr-Kasem et al., 2019), and impulsive-compulsive behavior (Tessitore et al., 2017). Our results showed that DBS partially reversed functional connectivity between FPN and DMN. This might be the reason that DBS has efficacy in the treatment of PD non-motor symptoms. In summary,

DBS demonstrated multi-network-modulated patterns with key nodes in SMN and FPN.

Our study identified the modulation of higher-order networks by DBS, which we speculated was mediated through the hyperdirect pathway (Polyakova et al., 2020). The hyperdirect pathway refers to direct projections between basal ganglia and cortex. The existence of a direct connection of fibers between these regions is the basis of this hypothesis. In PD, the hyperdirect pathway transmits excitatory stimuli from the motor, limbic, and associative brain regions (Quartarone et al., 2020). Electrophysiological studies confirm that β oscillation abnormalities are present in the basal ganglia-cortex circuits and are modulated by the STN-DBS (Oswal et al., 2021). Animal studies show that DBS can modulate motor control and mood disorders through hyperdirect pathway (Antonazzo et al., 2021; Nakata et al., 2021). These findings support the result of this study and provide a basis for further studies.

Previous research has shown that patients with PD had both ipsilateral and contralateral abnormal functional connectivities. Burman et al. (2014) reported that patients with PD showed a

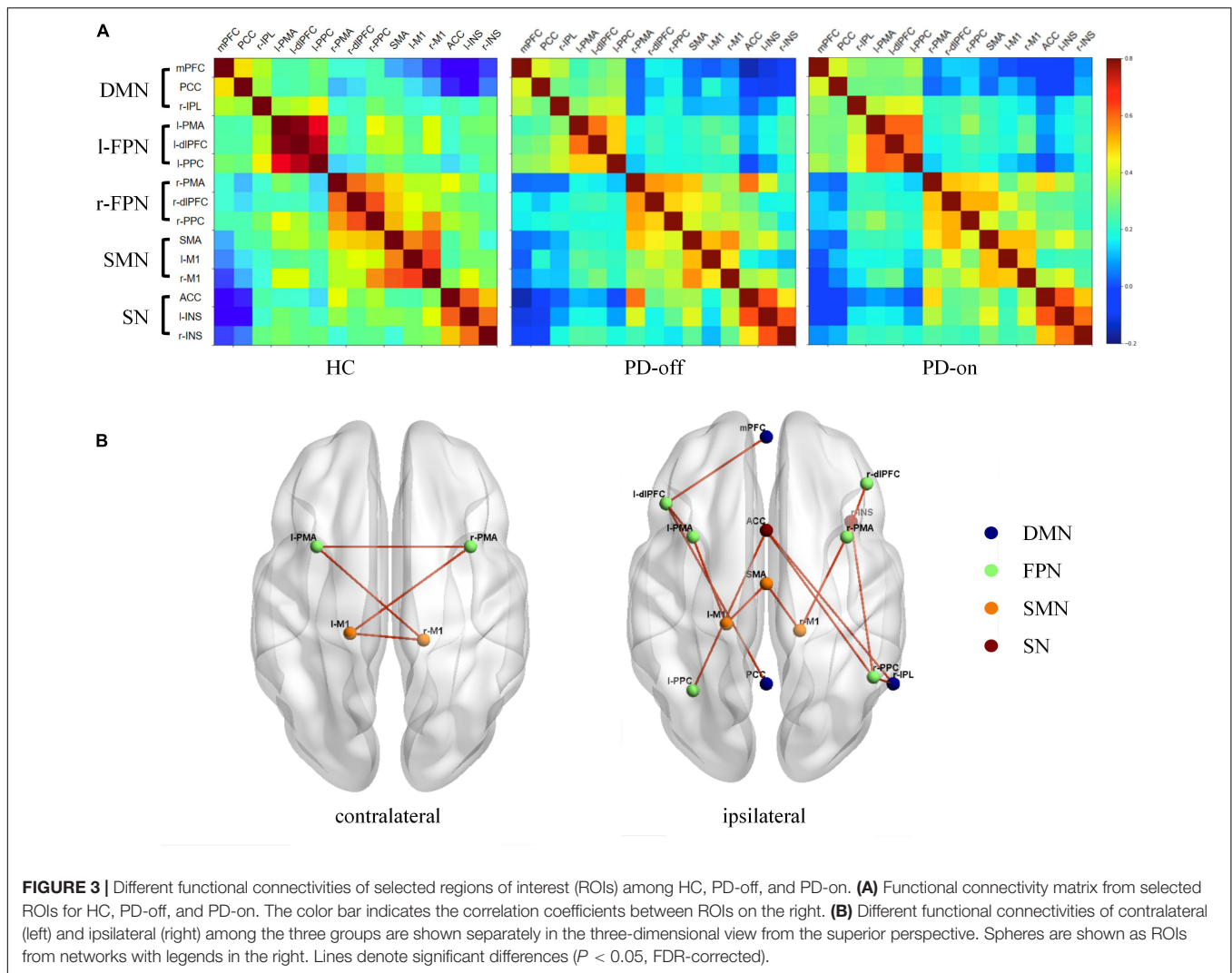
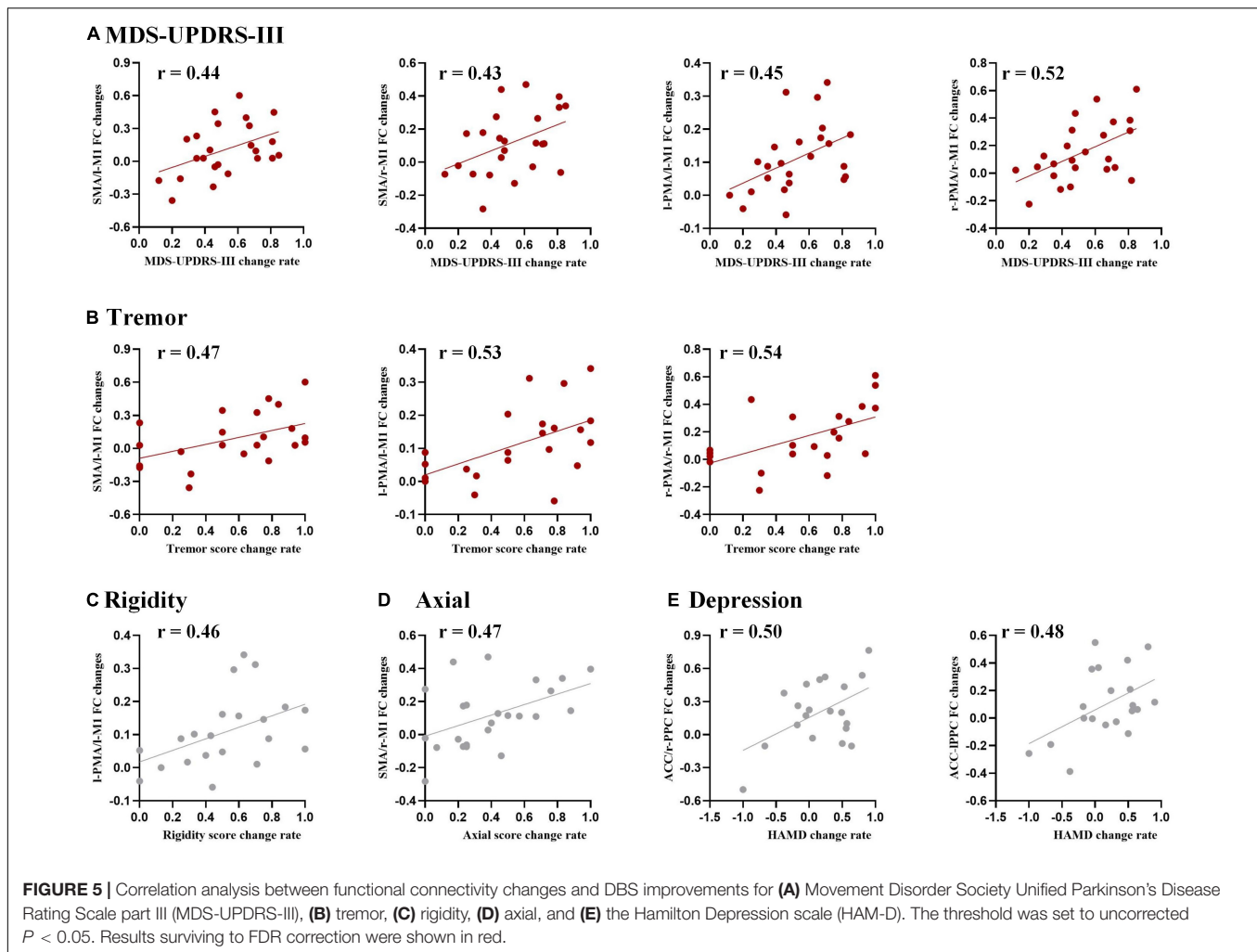


FIGURE 3 | Different functional connectivities of selected regions of interest (ROIs) among HC, PD-off, and PD-on. **(A)** Functional connectivity matrix from selected ROIs for HC, PD-off, and PD-on. The color bar indicates the correlation coefficients between ROIs on the right. **(B)** Different functional connectivities of contralateral (left) and ipsilateral (right) among the three groups are shown separately in the three-dimensional view from the superior perspective. Spheres are shown as ROIs from networks with legends in the right. Lines denote significant differences ($P < 0.05$, FDR-corrected).

significant decrease in functional connectivity across the bilateral hemispheres of M1 when compared with HC. Furthermore, Fiorenzato et al. (2019) described brain networks in PD as “segregated,” recognizing that PD showed a significant weakening of intra- and inter-network connections when compared with HCs, which involved nearly all intrinsic networks. We found that almost all changes in multiple functional connectivities in patients with PD were reduced when compared with HCs, confirming the results of previous studies. To the best of our knowledge, the PD brain networks modulated by DBS were generally limited to the ipsilateral network, with less evidence of cross-hemispheric modulations. In this study, we noted that DBS only modulated ipsilateral abnormal functional connectivity. One possible explanation was that DBS induced an unbalanced modulation. Evidence has shown that bilateral DBS was asymmetric in the treatment of motor symptoms, leading to overstimulation on one side and understimulation on the other side (Kahan et al., 2014). Furthermore, Zhang et al. (2020) conducted asymmetric lead implantation, with STN on one side and globus pallidus internus (GPI) on the other side, producing

satisfactory results. In summary, DBS demonstrated ipsilateral modulation patterns.

We further explored the correlations between the abnormal functional connectivity reversed by DBS and improvements in behavioral performance. It was interesting to note that the motor and depression were modulated by functional connectivity among different networks and that modulation heterogeneities existed even among different types of motor symptoms. (1) Improvement of all types of motor symptoms was related to functional connectivity changes within SMN and in FPN/SMN. The heterogeneity among symptoms may have arisen from neural remodeling caused by DBS, which gradually occurred. This process resulted in differences in improvement times among different motor symptoms (Krauss et al., 2004; de Hemptinne et al., 2015). Generally, tremor and rigidity improve in seconds to minutes, while axial often takes days to weeks to take effect (Ashkan et al., 2017). Moreover, Shen et al. (2020) reported that DBS modulated two distinct circles, namely, GPi and M1, which were associated with overall motor performance and bradykinesia, respectively. By employing volume tissue



(Smith et al., 2009; Allen et al., 2011). All networks were identical to the previously reported distributions of healthy individuals. In addition, the selection of ROI strictly avoided the areas of artifacts. Moreover, the potentially affected areas, such as the left inferior parietal lobule (l-IPL), were excluded for the ROI analysis. Finally, we did not acquire preoperative fMRI data and failed to perform a longitudinal analysis. Future studies can consider this design, which will bring more benefits in understanding the changed processes of functional connectivity induced by DBS.

CONCLUSION

This study found the modulation of DBS on multiple networks. Its changes were significantly correlated with the improvement of clinical symptoms. Specifically, DBS modulated the functional connectivity within SMN and across multiple networks centered by the FPN, and DBS was characterized by ipsilateral modulation patterns, with the patterns having inter-symptom differences. Overall, this study provided the basis for large-scale brain network research on multi-network DBS modulation.

DATA AVAILABILITY STATEMENT

The original contributions presented in the study are included in the article/**Supplementary Material**, further inquiries can be directed to the corresponding author/s.

ETHICS STATEMENT

The studies involving human participants were reviewed and approved by IRB of Beijing Tiantan Hospital. The patients/participants provided their written informed consent to participate in this study.

AUTHOR CONTRIBUTIONS

YB, YDi, and YJ contributed to conceptualization, data curation, formal analysis, investigation, software, visualization, and writing – original draft. LG, ZZ, ZY, DC, HF, and QZ contributed to methodology, visualization, writing, reviewing, and editing. TH, HX, and DW contributed to data curation. YDu, FM,

and YL contributed to supervision, project administration, writing, reviewing, and editing. JZ contributed to funding acquisition, project administration, resources, writing, reviewing, and editing. All authors contributed to the article and approved the submitted version.

FUNDING

This study was financially supported by the National Natural Science Foundation of China (81830033 and 61761166004).

REFERENCES

- Akram, H., Sotiropoulos, S. N., Jbabdi, S., Georgiev, D., Mahlknecht, P., Hyam, J., et al. (2017). Subthalamic deep brain stimulation sweet spots and hyperdirect cortical connectivity in Parkinson's disease. *Neuroimage* 158, 332–345. doi: 10.1016/j.neuroimage.2017.07.012
- Allen, E. A., Erhardt, E. B., Damaraju, E., Gruner, W., Segall, J. M., Silva, R. F., et al. (2011). A baseline for the multivariate comparison of resting-state networks. *Front. Syst. Neurosci.* 5:2. doi: 10.3389/fnsys.2011.00002
- Antonazzo, M., Gomez-Urquijo, S. M., Ugedo, L., and Morera-Herreras, T. (2021). Dopaminergic denervation impairs cortical motor and associative/limbic information processing through the basal ganglia and its modulation by the CB1 receptor. *Neurobiol. Dis.* 148:105214. doi: 10.1016/j.nbd.2020.105214
- Ashkan, K., Rogers, P., Bergman, H., and Ughratdar, I. (2017). Insights into the mechanisms of deep brain stimulation. *Nat. Rev. Neurol.* 13, 548–554. doi: 10.1038/nrneuro.2017.105
- Bejr-Kasem, H., Pagonabarraga, J., Martinez-Horta, S., Sampedro, F., Marin-Lahoz, J., Horta-Barba, A., et al. (2019). Disruption of the default mode network and its intrinsic functional connectivity underlies minor hallucinations in Parkinson's disease. *Mov. Disord.* 34, 78–86. doi: 10.1002/mds.27557
- Bronstein, J. M., Tagliati, M., Alterman, R. L., Lozano, A. M., Volkmann, J., Stefani, A., et al. (2011). Deep brain stimulation for Parkinson disease: an expert consensus and review of key issues. *Arch. Neurol.* 68, 165. doi: 10.1001/archneurol.2010.260
- Burman, K. J., Bakola, S., Richardson, K. E., Reser, D. H., and Rosa, M. G. (2014). Patterns of cortical input to the primary motor area in the marmoset monkey. *J. Comp. Neurol.* 522, 811–843. doi: 10.1002/cne.23447
- Calhoun, V. D., Adali, T., Pearlson, G. D., and Pekar, J. J. (2001). A method for making group inferences from functional MRI data using independent component analysis. *Hum. Brain Mapp.* 14:3. doi: 10.1002/hbm
- Cartmill, T., Skvarc, D., Bittar, R., McGillivray, J., Berk, M., and Byrne, L. K. (2021). Deep brain stimulation of the subthalamic nucleus in Parkinson's disease: a meta-analysis of mood effects. *Neuropsychol. Rev.* 31, 385–401. doi: 10.1007/s11065-020-09467-z
- Chen, L., Bedard, P., Hallett, M., and Horowitz, S. G. (2021). Dynamics of top-down control and motor networks in Parkinson's disease. *Mov. Disord.* 36, 916–926. doi: 10.1002/mds.28461
- de Hemptinne, C., Swann, N. C., Ostrem, J. L., Ryapolova-Webb, E. S., San Luciano, M., Galifianakis, N. B., et al. (2015). Therapeutic deep brain stimulation reduces cortical phase-amplitude coupling in Parkinson's disease. *Nat. Neurosci.* 18, 779–786. doi: 10.1038/nn.3997
- Diao, Y., Bai, Y., Hu, T., Yin, Z., Liu, H., Meng, F., et al. (2021). A meta-analysis of the effect of subthalamic nucleus-deep brain stimulation in Parkinson's disease-Related Pain. *Front. Hum. Neurosci.* 15:688818. doi: 10.3389/fnhum.2021.688818
- Dixon, M. L., De La Vega, A., Mills, C., Andrews-Hanna, J., Spreng, R. N., Cole, M. W., et al. (2018). Heterogeneity within the frontoparietal control network and its relationship to the default and dorsal attention networks. *Proc. Natl. Acad. Sci. U.S.A.* 115, E1598–E1607. doi: 10.1073/pnas.1715766115
- Fiorenzato, E., Strafella, A. P., Kim, J., Schifano, R., Weis, L., Antonini, A., et al. (2019). Dynamic functional connectivity changes associated with dementia in Parkinson's disease. *Brain* 142, 2860–2872. doi: 10.1093/brain/awz192
- Himberg, J., Hyvarinen, A., and Esposito, F. (2004). Validating the independent components of neuroimaging time series via clustering and visualization. *Neuroimage* 22, 1214–1222. doi: 10.1016/j.neuroimage.2004.03.027
- Holiga, S., Mueller, K., Moller, H. E., Urgosik, D., Ruzicka, E., Schroeter, M. L., et al. (2015). Resting-state functional magnetic resonance imaging of the subthalamic microlesion and stimulation effects in Parkinson's disease: indications of a principal role of the brainstem. *Neuroimage Clin.* 9, 264–274. doi: 10.1016/j.nicl.2015.08.008
- Horn, A., Wenzel, G., Irmen, F., Huebl, J., Li, N., Neumann, W. J., et al. (2019). Deep brain stimulation induced normalization of the human functional connectome in Parkinson's disease. *Brain* 142, 3129–3143. doi: 10.1093/brain/awz239
- Hu, X., Song, X., Yuan, Y., Li, E., Liu, J., Liu, W., et al. (2015). Abnormal functional connectivity of the amygdala is associated with depression in Parkinson's disease. *Mov. Disord.* 30, 238–244. doi: 10.1002/mds.26087
- Ji, G. J., Hu, P., Liu, T. T., Li, Y., Chen, X., Zhu, C., et al. (2018). Functional connectivity of the corticobasal ganglia-thalamocortical network in parkinson disease: a systematic review and meta-analysis with cross-validation. *Radiology* 287, 973–982. doi: 10.1148/radiol.2018172183
- Johnson, L. A., Wang, J., Nebeck, S. D., Zhang, J., Johnson, M. D., and Vitek, J. L. (2020). Direct activation of primary motor cortex during subthalamic but not pallidal deep brain stimulation. *J. Neurosci.* 40, 2166–2177. doi: 10.1523/JNEUROSCI.2480-19.2020
- Kahan, J., Mancini, L., Flandin, G., White, M., Papadaki, A., Thornton, J., et al. (2019). Deep brain stimulation has state-dependent effects on motor connectivity in Parkinson's disease. *Brain* 142, 2417–2431. doi: 10.1093/brain/awz164
- Kahan, J., Urner, M., Moran, R., Flandin, G., Marreiros, A., Mancini, L., et al. (2014). Resting state functional MRI in Parkinson's disease: the impact of deep brain stimulation on 'effective' connectivity. *Brain* 137(Pt 4), 1130–1144. doi: 10.1093/brain/awu027
- Keller, S. S., Glenn, G. R., Weber, B., Kreilkamp, B. A., Jensen, J. H., Helpert, J. A., et al. (2017). Preoperative automated fibre quantification predicts postoperative seizure outcome in temporal lobe epilepsy. *Brain* 140, 68–82. doi: 10.1093/brain/aww280
- Krauss, J. K., Lipsman, N., Aziz, T., Boutet, A., Brown, P., Chang, J. W., et al. (2021). Technology of deep brain stimulation: current status and future directions. *Nat. Rev. Neurol.* 17, 75–87. doi: 10.1038/s41582-020-00426-z
- Krauss, J. K., Yianni, J., Loher, T. J., and Aziz, T. Z. (2004). Deep brain stimulation for dystonia. *J. Clin. Neurophysiol.* 21, 18–30.
- Lam, T. K., Dawson, D. R., Honjo, K., Ross, B., Binns, M. A., Stuss, D. T., et al. (2018). Neural coupling between contralesional motor and frontoparietal networks correlates with motor ability in individuals with chronic stroke. *J. Neurol. Sci.* 384, 21–29. doi: 10.1016/j.jns.2017.11.007
- Lang, S., Hanganu, A., Gan, L. S., Kibreab, M., Auclair-Ouellet, N., Alrazi, T., et al. (2019). Network basis of the dysexecutive and posterior cortical cognitive profiles in Parkinson's disease. *Mov. Disord.* 34, 893–902. doi: 10.1002/mds.27674
- Lou, Y., Huang, P., Li, D., Cen, Z., Wang, B., Gao, J., et al. (2015). Altered brain network centrality in depressed Parkinson's disease patients. *Mov. Disord.* 30, 1777–1784. doi: 10.1002/mds.26321

ACKNOWLEDGMENTS

We thank all the subjects who participated in this study, and the MRI crew.

SUPPLEMENTARY MATERIAL

The Supplementary Material for this article can be found online at: <https://www.frontiersin.org/articles/10.3389/fnagi.2022.794987/full#supplementary-material>

- Mansouri, A., Taslimi, S., Badhiwala, J. H., Witiw, C. D., Nassiri, F., Odekerken, V. J. J., et al. (2018). Deep brain stimulation for Parkinson's disease: meta-analysis of results of randomized trials at varying lengths of follow-up. *J. Neurosurg.* 128, 1199–1213. doi: 10.3171/2016.11.JNS16715
- Manza, P., Zhang, S., Li, C. S., and Leung, H. C. (2016). Resting-state functional connectivity of the striatum in early-stage Parkinson's disease: cognitive decline and motor symptomatology. *Hum. Brain Mapp.* 37, 648–662. doi: 10.1002/hbm.23056
- Mohan, A., Roberto, A. J., Mohan, A., Lorenzo, A., Jones, K., Carney, M. J., et al. (2016). The significance of the default mode network (DMN) in neurological and neuropsychiatric disorders a review. *Yale J. Biol. Med.* 89, 49–57.
- Molnar, G. F., Sailer, A., Gunraj, C. A., Cunic, D. I., Lang, A. E., Lozano, A. M., et al. (2005). Changes in cortical excitability with thalamic deep brain stimulation. *Neurology* 64, 1913–1919. doi: 10.1212/01.WNL.0000163985.89444.DD
- Mueller, K., Jech, R., Ruzicka, F., Holiga, S., Ballarini, T., Bezdicek, O., et al. (2018). Brain connectivity changes when comparing effects of subthalamic deep brain stimulation with levodopa treatment in Parkinson's disease. *Neuroimage Clin.* 19, 1025–1035. doi: 10.1016/j.nicl.2018.05.006
- Nachev, P., Coulthard, E., Jager, H. R., Kennard, C., and Husain, M. (2008). Enantiomorphic normalization of focally lesioned brains. *Neuroimage* 39, 1215–1226. doi: 10.1016/j.neuroimage.2007.10.002
- Nakata, K. G., Yin, E., Sutlief, E., and Ferguson, S. M. (2021). Chemogenetic modulation reveals distinct roles of the subthalamic nucleus and its afferents in the regulation of locomotor sensitization to amphetamine in rats. *Psychopharmacology (Berl.)* 239, 353–364. doi: 10.1007/s00213-021-05985-7
- Oswal, A., Cao, C., Yeh, C. H., Neumann, W. J., Gratwicke, J., Akram, H., et al. (2021). Neural signatures of hyperdirect pathway activity in Parkinson's disease. *Nat. Commun.* 12, 5185. doi: 10.1038/s41467-021-25366-0
- Petry-Schmelzer, J. N., Krause, M., Dembek, T. A., Horn, A., Evans, J., Ashkan, K., et al. (2019). Non-motor outcomes depend on location of neurostimulation in Parkinson's disease. *Brain* 142, 3592–3604. doi: 10.1093/brain/awz285
- Polyakova, Z., Chiken, S., Hatanaka, N., and Nambu, A. (2020). Cortical control of subthalamic neuronal activity through the hyperdirect and indirect pathways in monkeys. *J. Neurosci.* 40, 7451–7463. doi: 10.1523/JNEUROSCI.0772-20.2020
- Quartarone, A., Cacciola, A., Milardi, D., Ghilardi, M. F., Calamuneri, A., Chillemi, G., et al. (2020). New insights into cortico-basal-cerebellar connectome: clinical and physiological considerations. *Brain* 143, 396–406. doi: 10.1093/brain/awz310
- Shen, L., Jiang, C., Hubbard, C. S., Ren, J., He, C., Wang, D., et al. (2020). Subthalamic Nucleus Deep Brain Stimulation Modulates 2 Distinct Neurocircuits. *Ann. Neurol.* 88, 1178–1193. doi: 10.1002/ana.25906
- Shi, Y., Zeng, Y., Wu, L., Liu, W., Liu, Z., Zhang, S., et al. (2017). A study of the brain abnormalities of post-stroke depression in frontal lobe lesion. *Sci. Rep.* 7:13203. doi: 10.1038/s41598-017-13681-w
- Smith, S. M., Fox, P. T., Miller, K. L., Glahn, D. C., Fox, P. M., Mackay, C. E., et al. (2009). Correspondence of the brain's functional architecture during activation and rest. *Proc. Natl. Acad. Sci. U.S.A.* 106, 13040–13045. doi: 10.1073/pnas.0905267106
- Stenmark Persson, R., Nordin, T., Hariz, G. M., Wardell, K., Forsgren, L., Hariz, M., et al. (2021). Deep brain stimulation of caudal zona incerta for Parkinson's disease: one-year follow-up and electric field simulations. *Neuromodulation* doi: 10.1111/ner.13500 [Epub ahead of print].
- Suo, X., Lei, D., Li, N., Cheng, L., Chen, F., Wang, M., et al. (2017). Functional brain connectome and its relation to hoehn and yahr stage in Parkinson disease. *Radiology* 285, 904–913. doi: 10.1148/radiol.2017162929
- Tessitore, A., De Micco, R., Giordano, A., di Nardo, F., Caiazzo, G., Siciliano, M., et al. (2017). Intrinsic brain connectivity predicts impulse control disorders in patients with Parkinson's disease. *Mov. Disord.* 32, 1710–1719. doi: 10.1002/mds.27139
- Thirion, B., Pinel, P., Meriaux, S., Roche, A., Dehaene, S., and Poline, J. B. (2007). Analysis of a large fMRI cohort: statistical and methodological issues for group analyses. *Neuroimage* 35, 105–120. doi: 10.1016/j.neuroimage.2006.11.054
- Tinaz, S. (2021). Functional connectome in Parkinson's disease and Parkinsonism. *Curr. Neurol. Neurosci. Rep.* 21:24. doi: 10.1007/s11910-021-01111-4
- Vervoort, G., Alaerts, K., Bengevoord, A., Nackaerts, E., Heremans, E., Vandenberghe, W., et al. (2016). Functional connectivity alterations in the motor and fronto-parietal network relate to behavioral heterogeneity in Parkinson's disease. *Parkinsonism Relat. Disord.* 24, 48–55. doi: 10.1016/j.parkrelis.2016.01.016
- Wichmann, T., and DeLong, M. R. (2016). Deep brain stimulation for movement disorders of basal ganglia origin: restoring function or functionality? *Neurotherapeutics* 13, 264–283. doi: 10.1007/s13311-016-0426-6
- Wu, C., Matias, C., Foltynie, T., Limousin, P., Zrinzo, L., and Akram, H. (2021). Dynamic network connectivity reveals markers of response to deep brain stimulation in Parkinson's disease. *Front. Hum. Neurosci.* 15:729677. doi: 10.3389/fnhum.2021.729677
- Yeo, B. T., Krienen, F. M., Chee, M. W., and Buckner, R. L. (2014). Estimates of segregation and overlap of functional connectivity networks in the human cerebral cortex. *Neuroimage* 88, 212–227. doi: 10.1016/j.neuroimage.2013.10.046
- Yin, Z., Bai, Y., Zou, L., Zhang, X., Wang, H., Gao, D., et al. (2021b). Balance response to levodopa predicts balance improvement after bilateral subthalamic nucleus deep brain stimulation in Parkinson's disease. *NPJ Parkinsons Dis.* 7:47. doi: 10.1038/s41531-021-00192-9
- Yin, Z., Bai, Y., Guan, B., Jiang, Y., Wang, Z., Meng, F., et al. (2021a). A quantitative analysis of the effect of bilateral subthalamic nucleus-deep brain stimulation on subjective and objective sleep parameters in Parkinson's disease. *Sleep Med.* 79, 195–204. doi: 10.1016/j.sleep.2020.10.021
- Yourganov, G., Fridriksson, J., Rorden, C., Gleichgercht, E., and Bonilha, L. (2016). Multivariate connectome-based symptom mapping in post-stroke patients: networks supporting language and speech. *J. Neurosci.* 36, 6668–6679. doi: 10.1523/JNEUROSCI.4396-15.2016
- Zhang, C., Lai, Y., Li, J., He, N., Liu, Y., Li, Y., et al. (2021). Subthalamic and pallidal stimulations in patients with Parkinson's disease: common and dissociable connections. *Ann. Neurol.* 90, 670–682. doi: 10.1002/ana.26199
- Zhang, C., Wang, L., Hu, W., Wang, T., Zhao, Y., Pan, Y., et al. (2020). Combined unilateral subthalamic nucleus and contralateral globus pallidus interna deep brain stimulation for treatment of parkinson disease: a pilot study of symptom-tailored stimulation. *Neurosurgery* 87, 1139–1147. doi: 10.1093/neuros/nyaa201

Conflict of Interest: The authors declare that the research was conducted in the absence of any commercial or financial relationships that could be construed as a potential conflict of interest.

Publisher's Note: All claims expressed in this article are solely those of the authors and do not necessarily represent those of their affiliated organizations, or those of the publisher, the editors and the reviewers. Any product that may be evaluated in this article, or claim that may be made by its manufacturer, is not guaranteed or endorsed by the publisher.

Copyright © 2022 Bai, Diao, Gan, Zhuo, Yin, Hu, Cheng, Xie, Wu, Fan, Zhang, Duan, Meng, Liu, Jiang and Zhang. This is an open-access article distributed under the terms of the Creative Commons Attribution License (CC BY). The use, distribution or reproduction in other forums is permitted, provided the original author(s) and the copyright owner(s) are credited and that the original publication in this journal is cited, in accordance with accepted academic practice. No use, distribution or reproduction is permitted which does not comply with these terms.